TRAF2 recruitment via T61 in CD30 drives NFκB activation and enhances hESC survival and proliferation

Nilay Y. Thakar[a], Dmitry A. Ovchinnikov[a], Marcus L. Hastie[b], Bostjan Kobe[c], Jeffrey J. Gorman[b], and Ernst J. Wolvetang[a]

[a]Stem Cell Engineering Group, Australian Institute for Bioengineering and Nanotechnology, University of Queensland, St. Lucia, QLD 4072, Australia; [b]Protein Discovery Centre, QIMR Berghofer Medical Research Institute, Herston, QLD 4029, Australia; [c]School of Chemistry and Molecular Biosciences, Australian Infectious Diseases Research Centre and Institute for Molecular Bioscience, University of Queensland, St. Lucia, 4067 QLD, Australia

ABSTRACT CD30 (TNFRSF8), a tumor necrosis factor receptor family protein, and CD30 variant (CD30v), a ligand-independent form encoding only the cytoplasmic signaling domain, are concurrently overexpressed in transformed human embryonic stem cells (hESCs) or hESCs cultured in the presence of ascorbate. CD30 and CD30v are believed to increase hESC survival and proliferation through NFκB activation, but how this occurs is largely unknown. Here we demonstrate that hESCs that endogenously express CD30v and hESCs that artificially overexpress CD30v exhibit increased ERK phosphorylation levels, activation of the canonical NFκB pathway, down-regulation of the noncanonical NFκB pathway, and reduced expression of the full-length CD30 protein. We further find that CD30v, surprisingly, resides predominantly in the nucleus of hESC. We demonstrate that alanine substitution of a single threonine residue at position 61 (T61) in CD30v abrogates CD30v-mediated NFκB activation, CD30v-mediated resistance to apoptosis, and CD30v-enhanced proliferation, as well as restores normal G_2/M-checkpoint arrest upon H_2O_2 treatment while maintaining its unexpected subcellular distribution. Using an affinity purification strategy and LC-MS, we identified TRAF2 as the predominant protein that interacts with WT CD30v but not the T61A-mutant form in hESCs. The identification of Thr-61 as a critical residue for TRAF2 recruitment and canonical NFκB signaling by CD30v reveals the substantial contribution that this molecule makes to overall NFκB activity, cell cycle changes, and survival in hESCs.

INTRODUCTION

CD30 (TNFRSF8) is a cancer-associated cell surface antigen and a member of the tumor necrosis factor receptor (TNFR) superfamily (Smith *et al.*, 1993; Gedrich *et al.*, 1996). It is a biomarker for malignant Reed–Sternberg cells in Hodgkin's disease (Durkop *et al.*, 1992), embryonal carcinoma (EC) cells (Durkop *et al.*, 2000), anaplastic large-cell lymphoma (ALCL) cells (Zheng *et al.*, 2003), in vitro–cultured aneuploid human embryonic stem cells (hESCs; Pera *et al.*, 1997; Herszfeld *et al.*, 2006), and hESCs and induced pluripotent stem cells cultured in the presence of ascorbate. A cryptic promoter in intron 10 of CD30 drives expression of CD30 variant (CD30v; Horie *et al.*, 1996), an mRNA that codes for only the cytoplasmic signaling tail of CD30 and is typically coexpressed with the full-length CD30 (CD30FL; Horie *et al.*, 1996, 1999), but, unlike CD30FL, CD30v does not require CD30 ligand (Horie *et al.*, 1996). In agreement with the observation that CD30FL and CD30v lack an intrinsic kinase domain,

homo-oligomerization of CD30FL or CD30v is believed to activate CD30 signaling through the recruitment of signal-transducing molecules such as members of the tumor necrosis factor receptor–associated factor (TRAF) family and the various TRAF-binding proteins (Horie *et al.*, 1999; Schneider and Hübinger, 2002). Previous deletion studies identified the extreme C-terminal 30 amino acids of CD30 as the domain responsible for interaction with TRAFs and subsequent NFκB activation (Gedrich *et al.*, 1996; Aizawa *et al.*, 1997; Horie *et al.*, 1998, 1999; Horie and Watanabe, 1998; Buchan and Al-Shamkhani, 2012) but also suggested contributions of more-N-terminal regions (Horie *et al.*, 1998; Wright and Duckett, 2009). The discovery that aryl hydrocarbon nuclear translocator (ARNT) interacts with the CD30 signaling domain and suppresses CD30-mediated NFκB signaling in KARPAS-299 cells through a negative feedback mechanism (Wright and Duckett, 2009) revealed that CD30 signaling is more complex than was initially appreciated (Horie *et al.*, 1998; Wright and Duckett, 2009). For example, the precise molecular mechanism underlying NFκB activation by CD30 remains largely to be elucidated (Gedrich *et al.*, 1996; Aizawa *et al.*, 1997; Horie *et al.*, 1998; Buchan and Al-Shamkhani, 2012). Here we show that the bulk of CD30v, somewhat unexpectedly, resides in the nucleus, and, using site-directed mutagenesis and proteomics approaches, we identify a single threonine residue at position 61 in CD30v that is critical for TRAF2 interaction, NFκB activation, and downstream CD30-NFκB–dependent phenotypes in hESCs. Our data offer an explanation for the often disparate results of CD30 domain–deletion studies and provide novel insight into the mechanism and roles(s) of CD30-dependent NFκB signaling in hESCs that it might be possible to exploit for hESC culture.

RESULTS

Thr-61 in CD30v is responsible for NFκB activation

Horie *et al.* (1998) showed that a novel D1 subdomain in CD30 comprising amino acids 500–538, constituting the first 39 amino acids of its cytoplasmic tail, was sufficient for NFκB activation and that this involved recruitment of a yet-to-be-identified TRAF protein but not TRAF2 or TRAF5. Our bioinformatic analysis suggested the presence of a putative fork-head associated (FHA) binding domain at amino acids 59–65 in CD30v (equivalent to amino acids 522–528 in full length [FL] CD30). We next created various mutant CD30v proteins with small deletions and point mutations within amino acids 59–65 of CD30v (Figure 1, A–C). Transient cotransfection of these mutant CD30v expression constructs with an NFκB luciferase reporter into HES3 hESCs revealed that deletion of amino acids 59–66 of CD30v (FHA CD30v Δ59–65) abrogated ~90% of NFκB activity in hESCs (Figure 1B). Cotransfection with an AP1-luciferase reporter showed for the first time that CD30v can activate AP1 signaling but also that deletion of residues 59–65 (CD30v Δ59–65) does not affect AP-1 activity, suggesting that this domain is specifically involved in NFκB activation downstream of CD30v (Figure 1B). In fact, no change in NFκB or AP1 activity was observed for any of the other CD30v mutants we generated (Figure 1B). We further report that, despite the bioinformatically predicted presence of putative sumoylation motifs, CD30v is not subject to SUMOylation (Supplemental Figure S1A). To determine the specific amino acid residues within the deleted region of CD30v that are responsible for NFκB activation, we mutated two putatively phosphorylatable threonine residues, one at position 61 (T61; Thr-524 in FL CD30) and one at position 66 (T66; Thr-529 in FL CD30), to alanine (T61A, T66A). Altering T61 (T61A CD30v), but not T66, to alanine significantly reduced the NFκB luciferase reporter activity to

near-background levels, indicating that T61 is critical for NFκB activation by CD30v (Figure 1C).

Thr-61 in CD30v is critical for CD30v–TRAF2 interaction

To understand better the role that CD30v plays in hESC biology and identify candidate proteins interacting with this threonine (possibly a novel TRAF protein as suggested by Horie *et al.*, 1998), we established HES3 hESCs that stably overexpress hemagglutinin (HA)-tagged wild-type CD30v (WT) and T61A mutant (T61A) proteins. As controls, we generated hESCs that contain an empty vector (OE V/C) or vector overexpressing enhanced green fluorescent protein (EGFP). Generation and maintenance of stable lines were performed in a standard hESC medium (NutriStem) that contains ascorbate, resulting in expression of endogenous CD30FL and CD30v proteins alongside artificially overexpressed HA-tagged wild-type or mutant CD30v proteins.

Western blot analysis revealed that T61 mutant and WT CD30v were overexpressed to similar levels (~20-fold; Figure 2, A and B). We reported earlier (Chung *et al.*, 2010b) that CD30v overexpression leads to *CD30FL* mRNA down-regulation and now show that this also leads to a decrease in CD30FL protein levels, consistent with the idea of existence of a negative-feedback mechanism by CD30 signaling (Figure 2, A and C). Of note, because this mechanism is observed in both WT and T61A CD30v proteins, we conclude that this negative-feedback mechanism likely occurs independently of the T61-driven NFκB activation.

Previous studies assumed that, like CD30FL, the shorter, ligand-independent CD30v would be located extranuclearly. However, when we performed nuclear-cytoplasmic fractionation of GFP, WT, and T61A cells, we found both WT and T61A CD30v predominantly in the nuclear fraction that contained the majority of Histone-H3 and the entire OCT4 transcription factor expression and to a smaller extent in the cytosolic fraction containing glyceraldehyde-3-phosphate dehydrogenase (GAPDH). As shown in Figure 2D, immunostaining with anti-HA antibody further confirmed the predominantly nuclear localization of both WT and T61A-mutant HA-tagged CD30v proteins (Figure 2E). Immunostaining with anti-TRAF2 antibody (Figure 2D) showed that whereas TRAF2 is predominantly cytoplasmic, a small proportion of TRAF2 is also present in the nucleus (Figure 2E). We thus conclude that in hESCs, CD30v is a predominantly nuclear protein and that mutation of Thr-61 does not interfere with its subcellular localization.

We next examined the effect of WT and T61A CD30v expression on the expression of NFκB proteins and NFκB target genes. WT CD30v overexpression leads to an increase in transcription of canonical NFκB proteins *RELA* and *NFκB1* and its downstream targets *BNIP3* and *VCAM1* and a concomitant decrease in levels of the noncanonical NFκB *RELB* gene (Supplemental Figure S1B). Conversely, expression of the mutant T61A CD30v protein, in agreement with its impaired NFκB-activating potential, displays no increase in *RELA*, *NFκB1*, or *BNIP3* and a decrease in *VCAM1* expression, with BNIP3 and VCAM1 being bona fide RELA targets (Supplemental Figure S1B).

To identify the protein that interacts with T61 and drives CD30-mediated NFκB activation, we immunoprecipitated HA-tagged proteins and their interacting partners with an anti-HA antibody and analyzed interacting proteins via liquid chromatography–mass spectrometry (LC-MS). EGFP-expressing hESCs were used to assess nonspecific protein interactions. Using this approach, we discovered that TRAF2 interacts with WT CD30v protein but not with the T61A-mutant CD30v (Supplemental Table S3). This was subsequently validated using Western blot analysis (Figure 3A). These data strongly
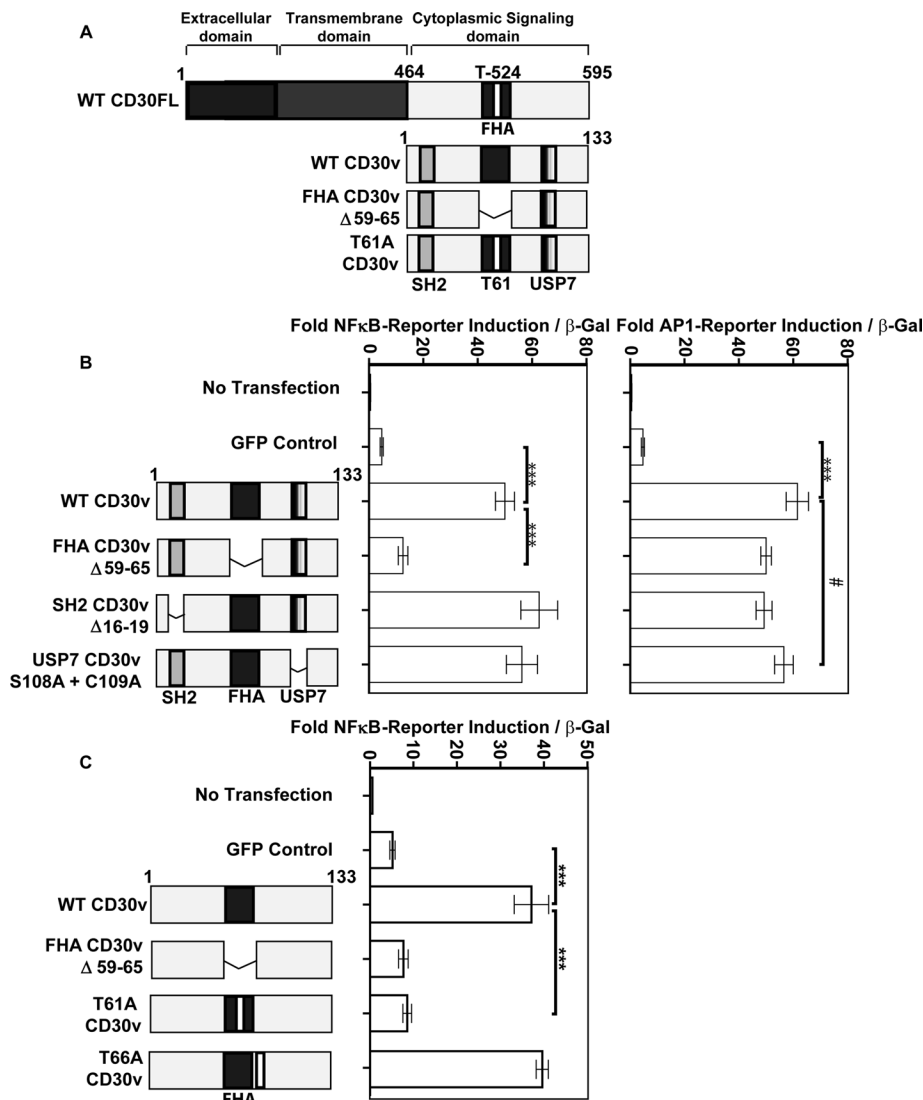
FIGURE 1: Thr-61 of CD30v is required for activation of NFκB signaling. (A) Graphical representation of the full-length CD30 (WT CD30FL) protein, highlighting Thr-524 within its cytoplasmic signaling domain. Wild-type (WT CD30v OE) and various mutant CD30v proteins highlighting Thr-61, which corresponds to Thr-524 within CD30 FL, are shown. (B) Measurement of NFκB and AP1 reporter activity via luciferase assay in HES3 hESCs transiently transfected with WT CD30v OE and mutant CD30v OE proteins. Schematics of the overexpressed WT and mutant CD30v proteins are shown next to reporter activity readings. Nontransfected and GFP-transfected cells were used as controls. The data are shown as mean fold changes ± SD of three independent experiments (#not significant, *$p < 0.05$, **$p < 0.01$, ***$p < 0.001$). (C) Measurement of NFκB activity via luciferase reporter assay in HES3 hESCs transiently-transfected with wild-type (WT CD30v OE) and mutant CD30v OE proteins. Graphical representation of the WT and mutant CD30v OE proteins. Nontransfected and GFP-transfected cells were used as controls. The data are shown as mean fold changes ± SD of three independent experiments (#not significant, *$p < 0.05$, **$p < 0.01$, ***$p < 0.001$).

suggest that T61 is critical for interaction of CD30v with TRAF2 and downstream NFκB signaling. We next verified that mutation of T61 itself did not alter TRAF2 mRNA or protein expression (Figure 2A and Supplemental Figure S1B) or its intracellular localization (Figure 2E).

To confirm further the role of TRAF2 recruitment via T61 in CD30v-driven NFκB activation, we down-regulated TRAF2 expression using TRAF2 small interfering RNAs (siRNAs) in HES3 hESCs overexpressing T61A CD30v, or a WT or an empty vector (OE V/C) as controls, and analyzed NFκB activity using a NFκB-luciferase reporter. TRAF2 siRNA treatment caused a significant reduction in

TRAF2 expression after 96 h as compared with GFP-targeting control siRNA (siGFP)–treated cells (Figure 3B). siTRAF2-treated WT CD30vOE hESCs displayed ~50% reduction in NFκB-reporter activity as compared with siGFP-treated CD30vOE hESCs (Figure 3C). TRAF2 siRNA treatment of hESCs expressing T61A-mutant CD30v further reduced the already low NFκB reporter activity to background levels (Figure 3C). We conclude that CD30v expression makes a substantial contribution to NFκB activity in hESCs and that this is in large part mediated by interaction of TRAF2 with T61 in CD30v.

TRAF2-mediated, T61-dependent NFκB signaling by CD30v accelerates cell cycle progression of hESCs

After the establishment of several independent WT and T61A-mutant CD30v-overexpressing hESC lines, we consistently observed significantly higher cell numbers in WT CD30v cells compared with the CD30v (T61A) mutant or control vector–transfected cells (Figure 4A). Cell cycle analysis indeed revealed a significant increase in percentage of cells in S phase (~10% increase) accompanied by a reduction in G_0/G_1 (by ~4%) and G_2/M (by ~6%) phases in WT CD30v-expressing hESCs as compared with the T61A mutant or the vector-only control cells (Figure 4B and Supplemental Figure S2A). Analysis of phospho–Histone H3 (Ser-10) levels, a marker of mitotic cells, indicated that hESCs that overexpress WT CD30v display a significantly lower (~2.8%) fraction of cells in M phase as compared with the T61A mutant, parental, and vector-only controls (3.7%; Figure 4C and Supplemental Figure S2B). This apparent increased cell cycle transition of CD30v-overexpressing cells was accompanied by a significant increase in *C-MYC*, *C-FOS*, *CYCLIN A2*, *CYCLIN E1*, *LIN28A*, and *CDC25A* expression, a decrease in *p27* expression (Figure 4D), but unchanged *CYCLIN D1*, *CYCLIN D2*, *CYCLIN D3*, and *p53* mRNA expression (Figure 4D). The observation that these cell cycle–related changes were not observed in the CD30v (T61A) mutant lines suggests that canonical NFκβ signaling via the interaction of TRAF2 with T61 in CD30 likely underlies the increased cell cycle progression in hESC and altered cell cycle regulation in CD30v-expressing hESCs.

Mutation of Thr-61 in CD30v interferes with CD30v-conferred inhibition of apoptosis and H_2O_2-induced G_2 cell cycle arrest

Because we previously reported that CD30FL (Herszfeld *et al.*, 2006) and CD30v overexpression (Chung *et al.*, 2010b) enhances hESC survival, we next investigated whether interference with CD30-mediated canonical NFκB activation in the Thr-61-mutant
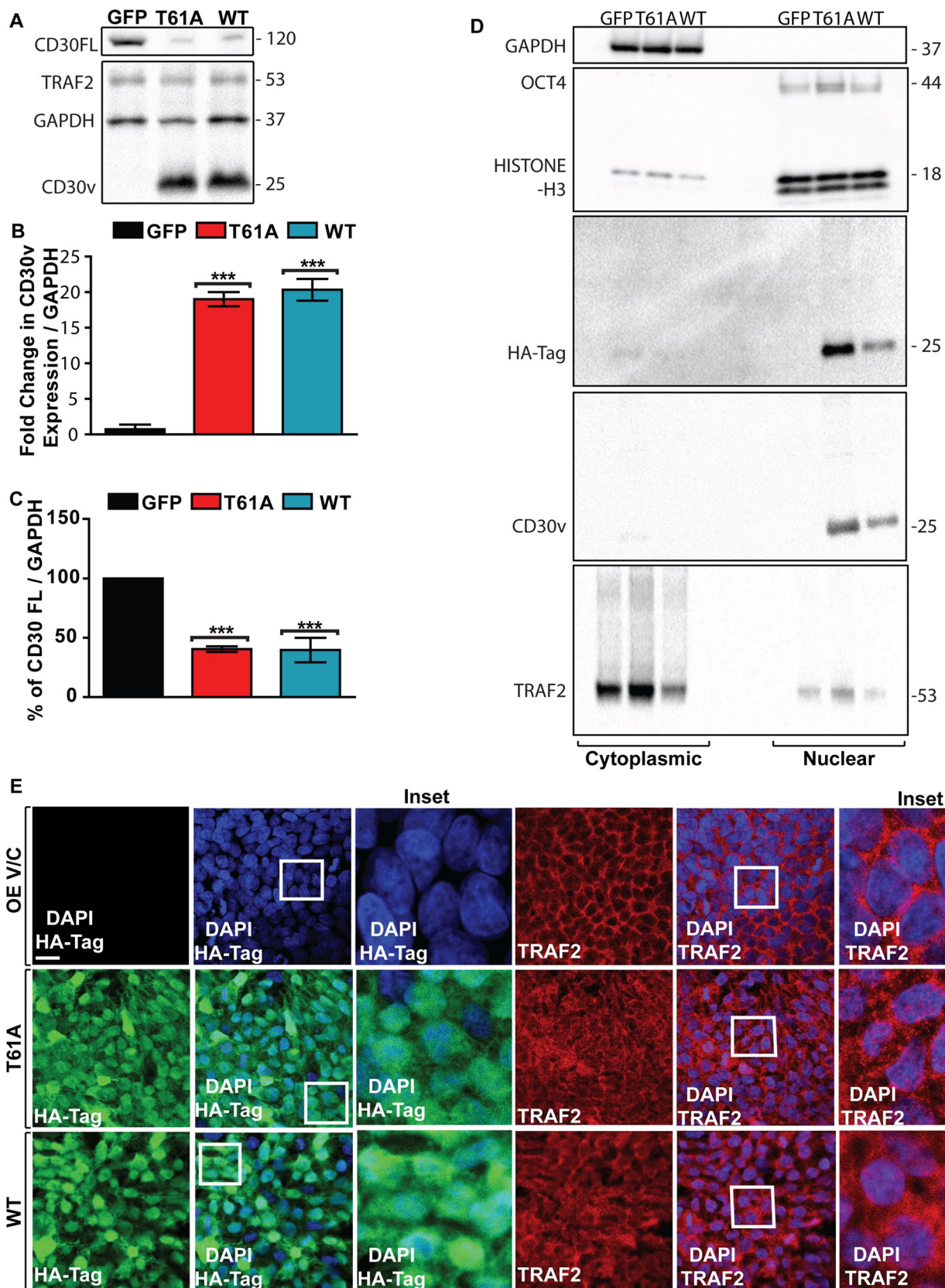
FIGURE 2: CD30v is localized predominantly in the nucleus. (A) HES3 hESCs that stably overexpress GFP (control), WT, or T61A mutant CD30v proteins were established and validated by Western blotting with CD30v antibody. CD30FL and TRAF2 expression was also detected. (B) Average densitometric quantification, indicating fold change in CD30v expression normalized to GAPDH in WT and T61A CD30v–expressing hESCs compared with GFP hESCs. This was carried out using Image Lab Analysis Software (Bio-Rad). The data represent the mean fold changes ± SD of three
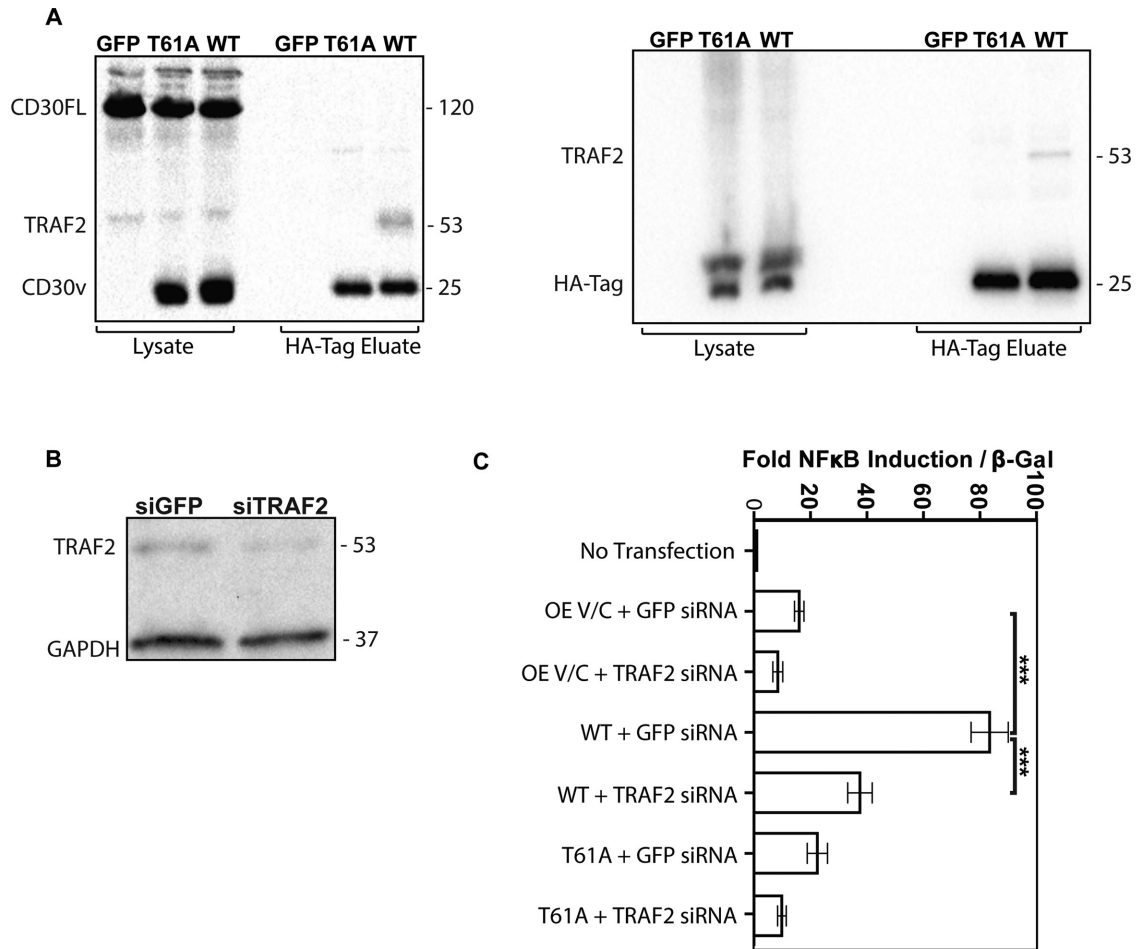
FIGURE 3: TRAF2 interacts with CD30v via T61 to drive CD30v-mediated NFκB activation. (A) Validation of immunoprecipitation and LC-MS experiment in WT and T61A hESCs as compared with GFP hESCs, using Western blot analysis for TRAF2. CD30 (left blot) and HA tag (right blot) were used as loading controls. TRAF2, CD30, and HA tag expression detected in lysates of GFP, T61A, and WT cells was compared with their respective expression in HA-tag eluates from these cells after immunoprecipitation. (B) Validation of knockdown of TRAF2 in hESCs using siRNA targeted against *TRAF2* mRNA (siTRAF2) using Western blot analysis. GFP siRNA (siGFP)–treated cells were used as a control. (C) Measurement of NFκB activity via luciferase assay in HES3 hESCs transiently cotransfected with overexpression vector control (OE V/C), WT, and T61A CD30v constructs and either siGFP or siTRAF2. Nontransfected cells (to detect background signal), OE V/C–transfected cells (to detect basal NFκB activity levels), and anti-GFP siRNA–transfected cells (to control for nonspecific siRNA effects) were used as controls to compare with NFκB activity in TRAF2 siRNA–treated cells. The data are shown as mean fold changes ± SD of three independent experiments (#not significant, *$p < 0.05$, **$p < 0.01$, ***$p < 0.001$).

CD30v-overexpressing cells affected cell survival. To this end, we subjected vector control, T61A, and WT cells to 200 μM H_2O_2 for 3 h as previously performed (Herszfeld *et al.*, 2006) and examined CASPASE-3 activation by immunofluorescence assay. As shown in Figure 5A, mutation of Thr-61 essentially abolished the ability of CD30v to inhibit H_2O_2-induced CASPASE-3 activation. Propidium

iodide (PI) staining of these same cell lines after challenge with 100 μM H_2O_2 for 24 h confirmed that WT-CD30v expression effectively inhibits the accumulation of apoptotic cells in the sub-G_0/G_1 region and that mutation of Thr-61 abolishes this antiapoptotic effect of WT CD30v (Figure 5B and Supplemental Figure S2C). Our data further show that whereas WT CD30v-overexpressing cells

independent experiments (#not significant, *$p < 0.05$, **$p < 0.01$, ***$p < 0.001$). (C) Average densitometry quantification indicating percentage of CD30FL expression normalized to GAPDH in WT and T61A compared with GFP hESCs. Quantification was carried out using Image Lab Analysis Software. The data are shown as mean fold changes ± SD of three independent experiments (#not significant, *$p < 0.05$, **$p < 0.01$, ***$p < 0.001$). (D) Nuclear-cytoplasmic fractionation was performed on the GFP, T61A, and WT HES3 hESCs, followed by Western blotting with antibodies against GAPDH (cytoplasmic marker), OCT4, and Histone-H3 (nuclear marker), HA tag, CD30v, and TRAF2. Representative Western blots of two independent experiments. (E) Intracellular localization of CD30v (HA tag) and TRAF2 was also observed using confocal microscopy. Cells were stained simultaneously for nuclear DNA (DAPI). Scale bar, 5 μm. Inset images (for white squares) are displayed for DAPI + HA tag and DAPI-TRAF2 staining. The images are representative of at least three independent experiments.
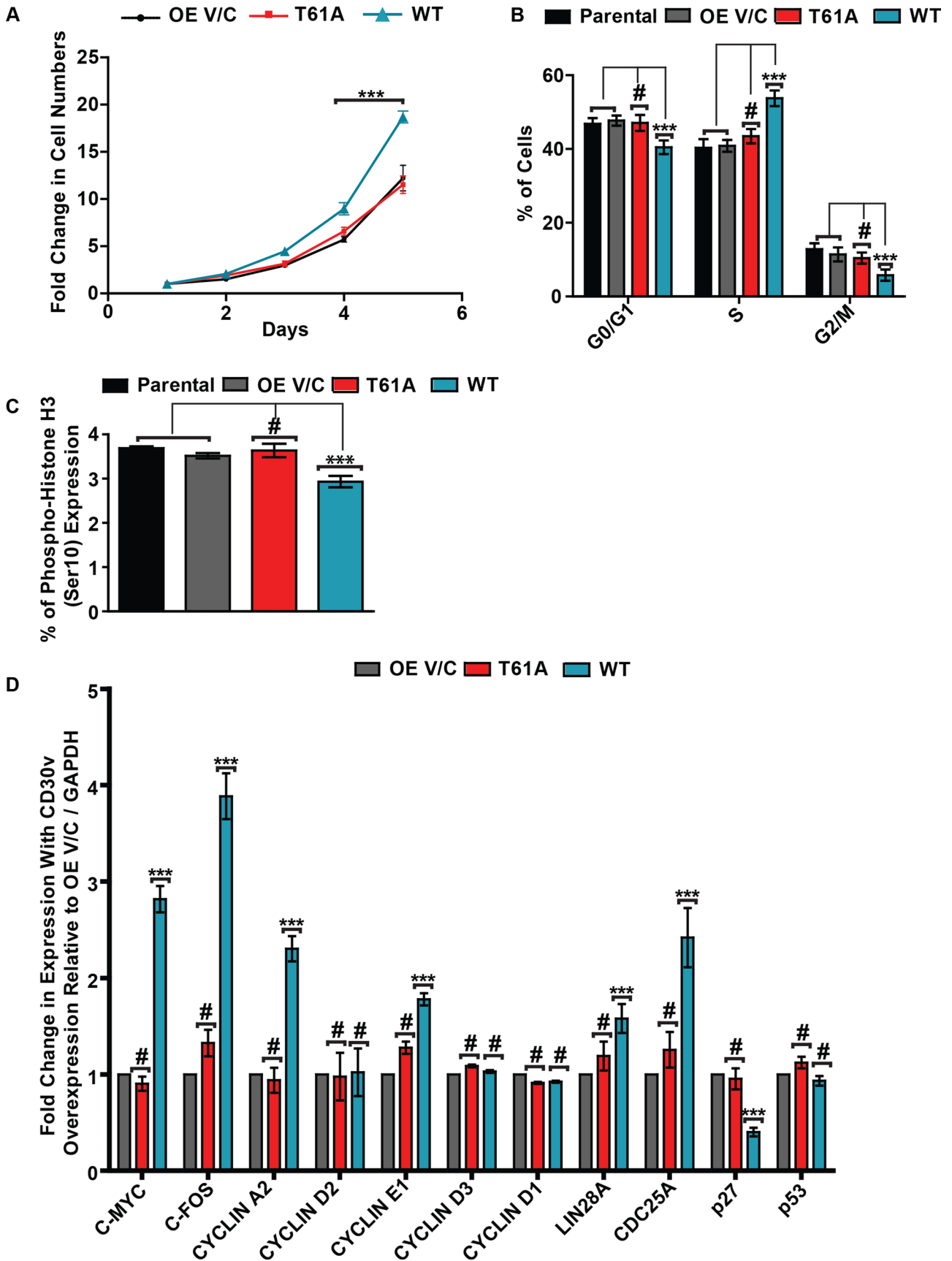
FIGURE 4: CD30v overexpression enhances hESC proliferation. (A) Fold change in cell numbers was measured over 5 d postseeding of WT and T61A cells as compared with OE V/C cells. The data are shown as mean fold changes ± SD of three independent experiments (#not significant, *$p < 0.05$, **$p < 0.01$, ***$p < 0.001$). (B) Cell cycle profile assessment of
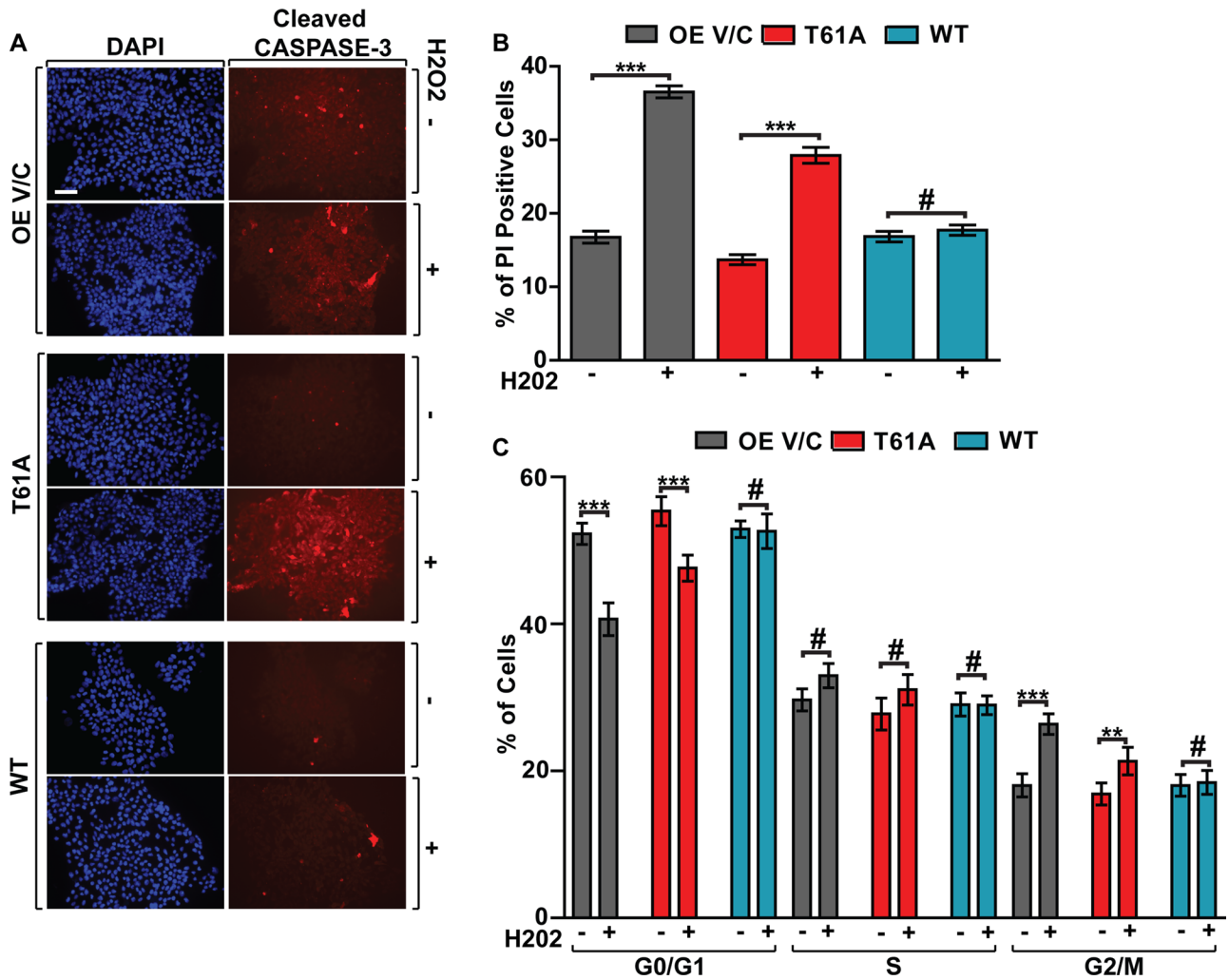
FIGURE 5: CD30v overexpression ameliorates H_2O_2-induced G2 cell cycle arrest. (A) Immunofluorescence analysis of active-CASPASE 3 in GFP, T61A, and WT hESCs that were either untreated or treated with 200 μM H_2O_2 for 3 h. Cells were stained simultaneously for nuclear DNA (DAPI). Scale bar, 10 μm. The images are representative of at least three independent experiments. (B) Percentage of dead cells (PI-positive cells using intact cell flow cytometry) in WT and T61A cells as compared with OE V/C cells after treatment with 100 μM H_2O_2 for 24 h. Cells not treated with H_2O_2 were used as controls. The data represent mean fold changes ± SD of three independent experiments (#not significant, *$p < 0.05$, **$p < 0.01$, ***$p < 0.001$). (C) Cell cycle profile assessment in WT and T61A cells as compared with OE V/C cells using samples obtained from B was carried out as per manufacturer's instructions using BD Cycletest Plus DNA Reagent Kit (BD Biosciences). The data represent mean fold changes ± SD of three independent experiments (#not significant, *$p < 0.05$, **$p < 0.01$, ***$p < 0.001$).

display no significant change in G_2/M or G_0/G_1 cell cycle after H_2O_2 challenge (Figure 5C and Supplemental Figure S2C), mutation of Thr-61 restores the ability of hESC to undergo H_2O_2-induced G_2/M-phase arrest, leading to a significant decrease in the G_0/G_1 population (Figure 5C and Supplemental Figure S2C), signifying that this occurs through a TRAF2-canonical NFκβ signaling cascade–dependent mechanism.

CD30v activates canonical NFκB and extracellular signal–regulated kinase signaling in hESCs

AP1 lies downstream of the extracellular signal–regulated kinase (ERK) signaling pathway, and CD30 is known to modulate ERK signaling in Hodgkin's lymphoma (HL) cell lines (Zheng et al., 2003; Watanabe et al., 2011). Because we observed that CD30v is predominantly nuclear and enhances AP1 activity independently of

---

untransduced, OE V/C, and T61A- and WT- CD30v–overexpressing cells carried out as per manufacturer's instructions using BD Cycletest Plus DNA Reagent Kit (BD Biosciences). The data are shown as mean ± SD of three independent experiments (#not significant, *$p < 0.05$, **$p < 0.01$, ***$p < 0.001$). (C) Phospho–Histone H3 (Ser-10) expression levels were measured using flow cytometry to determine the percentage of cells undergoing mitosis in parental, OE V/C, and T61A- and WT-CD30v–overexpressing cells. The data represent mean fold changes ± SD of three independent experiments (#not significant, *$p < 0.05$, **$p < 0.01$, ***$p < 0.001$). (D) mRNA expression analysis of various cell cycle regulators in T61A- and WT-CD30v–overexpressing cells as compared with OE V/C cells relative to GAPDH. The data represent mean fold changes ± SD of three independent experiments (#not significant, *$p < 0.05$, **$p < 0.01$, ***$p < 0.001$).

the T61/TRAF2-driven NFκβ-activation cascade, we hypothesized that a novel CD30-interacting protein may be involved in the AP1 or ERK activation cascade and its nuclear translocation. To this end, we used HES2 and HES4 hESCs grown in Knock-Out Serum Replacement (KOSR) minus ascorbate medium, allowing us to study CD30v-mediated effects in cells that are free of any endogenous CD30FL or CD30v expression. We described this culture method earlier (Chung et al., 2010b); however, the generation and maintenance of stable lines in ascorbate-free medium is very cumbersome.

We first examined the NFκβ pathway in two different hESC lines—HES2 (Supplemental Figure S3, A and B) and HES4 (Supplemental Figure S4, A and B)—that are completely free of endogenous CD30FL and CD30v expression as verified by immunostaining. We observed that in CD30v-overexpressing cells (CD30v[OE]), there is a substantial increase in canonical NFκβ signaling components—RELA, phospho-RELA (S-529), p105, and p50—whereas the noncanonical proteins RELB, NIK, p100, and p52 are down-regulated compared with CD30^{−} hESCs (no CD30FL or CD30v expression), indicating an opposing relationship between these pathways and further substantiating the notion that these are direct effects of CD30v-mediated NFκβ signaling.

We also examined the intracellular localization of CD30 proteins (both CD30FL and CD30v) in HES2 CD30[Endo] (Supplemental Figure S3C) and HES4 CD30[Endo] (Supplemental Figure S4C) hESCs grown in normal KOSR medium that contains ascorbate and hence triggers endogenous expression of both CD30FL and CD30v, and again we found a predominantly nuclear localization of CD30v, further substantiating that this phenotype is not an artifact arising from artificially overexpressing CD30v.

Finally, we examined expression and phosphorylation of ERKs in CD30^{−} and CD30v[OE] HES2 hESCs. Western blot analysis (Supplemental Figure S5, A and B) reveals that P-ERK (Thr-202/Tyr-204) levels are 1.5- to 2-fold higher in CD30v[OE] hESCs than in CD30^{−} cells without affecting total ERK expression. We conclude that CD30v signaling activates canonical NFκβ and ERK signaling. The CD30 domain responsible for ERK activation remains to be identified.

DISCUSSION

Deciphering how NFκβ and ERK signaling pathways govern survival, self-renewal, and pluripotency in human pluripotent stem cells is important for the development of safer culture conditions and their future application in regenerative medicine. CD30 is expressed in cells that are karyotypically abnormal, in hESCs exposed to ascorbate (Chung et al., 2010b), and its overexpression and constitutive NFκβ activation are the hallmarks of human germ cell tumors, embryonal carcinoma cells, and malignant Hodgkin Reed–Sternberg cells and ALCL (Durkop et al., 1992, 2000; Horie et al., 1996, 1998, 1999, 2002; Horie and Watanabe, 1998; Aizawa et al., 1997; Pera et al., 1997; Herszfeld et al., 2006; Amin and Lai, 2007; Hirsch et al., 2008; Harrison et al., 2009).

The role of CD30 and particularly NFκβ signaling in driving pathological phenotypes in HL and ALCL and its precise role in enhancing survival of hESCs have been a matter of debate (Armstrong et al., 2006). Several studies report that elevated levels of the CD30FL and CD30v, the ligand-independent shorter isoform of CD30, which is usually coexpressed with the full-length receptor, induce canonical and noncanonical NFκβ, AKT, and ERK activation via interaction with TRAFs to enhance survival, proliferation, and transformation of HL and ALCL cells (Durkop et al., 1992, 2000; Smith et al., 1993; Gedrich et al., 1996; Horie et al., 1996, 1998, 1999, 2002; Horie and Watanabe, 1998; Aizawa et al., 1997; Pera et al., 1997; Zheng et al., 2003; Nonaka et al., 2005; Watanabe

et al., 2005, 2011; Herszfeld et al., 2006; Amin and Lai, 2007; Wright and Duckett, 2009; Chung et al., 2010b; Buchan and Al-Shamkhani, 2012). Others, however, report that CD30 expression does not alter NFκB signaling or cause pathological effects in HL and decreases proliferation in ALCL cells (Wright et al., 2007; Hirsch et al., 2008). In hESCs, canonical and noncanonical NFκB signaling act in an opposing manner, and canonical NFκB signaling enhances survival of hESCs (Hat et al., 2009; Yang et al., 2010).

Previous studies in HL and ALCL cells indicated that the C-terminal 30 amino acids of CD30 were responsible for the interaction with TRAFs and subsequent CD30-dependent NFκB activation but that a yet-unidentified upstream signaling domain also plays a role (Gedrich et al., 1996; Aizawa et al., 1997; Horie et al., 1998; Buchan and Al-Shamkhani, 2012). When we interrogated the entire cytoplasmic tail of CD30 for the presence of potential signaling domains, we identified a 7-amino acid putative FHA domain–binding motif (residues 59–65), well away from the extreme C-terminus, which upon deletion abrogated all NFκB signaling activity mediated by CD30v. Replacement of individual amino acids within and around this domain with alanine revealed that mutation of a single Thr-61 to alanine in CD30v prevents >90% of NFκB activation by CD30v. Immunoprecipitation of HA-tagged CD30v from hESCs followed by LC-MS next revealed that recruitment of TRAF2, a known CD30-interacting and NFκB-activating protein, requires Thr-61 for interaction with CD30v. This suggests that mutation of Thr-61, a site potentially subject to phosphorylation (not tested in this study), interferes with TRAF2 recruitment to the more-C-terminal domains, perhaps by altering its conformation. The CD30 cytoplasmic tail (CD30v) sequence is predicted to be intrinsically unstructured (Kozlowski and Bujnicki, 2012) and shows limited similarity to any protein of known structure, suggesting that it may only adopt a defined structure when binding with interacting signaling proteins. The only structural information available for CD30 is for an 8-residue fragment (residues 576–583 of CD30/113-120 of CD30v) bound to TRAF2 (Ye et al., 1999). In this structure, the peptide binds in an extended conformation to the outer surface of the trimer of the TRAF-C domain of TRAF2. A 20-residue fragment from the cytoplasmic domain of CD40, the most closely related relative to CD30, complexed with the TRAF domain of TRAF3 shows that the CD40 fragment binds as a hairpin loop across the surface of the TRAF domain (Ni et al., 2000). We constructed a homology model (Eswar et al., 2008) of the analogous 21-residue peptide corresponding to the C-terminal region of CD30 (residues 574–594 of CD30/residues 111–131 of CD30v) bound to TRAF2 (Supplemental Figure S6). Although this model shows why the extreme C-terminus is important for TRAF2 binding and can explain why these fragments can independently bind TRAF2 in the absence of the rest of the CD30 cytoplasmic tail, it cannot explain why mutation of Thr-61/Thr-259 located some 50 residues N-terminally to this TRAF2-binding region at the C-terminus of CD30v is so critical. In the absence of cocrystallization of the full cytoplasmic domain of CD30 and TRAF2, we can only speculate that this site imparts important conformational cues that allow presentation of these domains. Alternatively, it is possible that the Thr-61 site interacts with a spatially adjacent region of TRAF2 and that this initial event is critical in providing structure to the CD30 C-terminus and enables subsequent TRAF2-binding events in the context of the full-length cytoplasmic domain. Because CD30v is known to interact with the same set of proteins as CD30FL and similarly induces ERK, AKT, and NFκB activation in a range of cell types (Smith et al., 1993; Aizawa et al., 1997; Horie and Watanabe, 1998; Horie et al., 2002; Watanabe et al., 2005; Wright et al., 2007), we hypothesize that Thr-61 has an equally critical role in TRAF2-dependent NFκB activation in CD30FL

as in CD30v. Remarkably, NFκB-reporter assays combined with siRNA knockdown of TRAF2 in hESC lines stably expressing T61mutant or WT CD30v indicate that the majority of TRAF2-mediated activation of NFκB signaling in hESC occurs through CD30v in a T61-dependent manner, highlighting the importance of CD30v and CD30FL expression for hESC biology.

Surprisingly, we detected a majority of CD30v in the nucleus of hESCs, a phenomenon that is not affected by the mutation of Thr-61. This raises the question as to how CD30v activates NFκB. We can envisage three possible scenarios: 1) the small amount of cytoplasmic CD30v leads to constitutive activation of the canonical TRAF2–IκB kinase (IKK)–NFκB pathway independently of CD30 ligand, 2) the TRAF2-CD30v cytoplasmic interaction facilitates CD30v nuclear accumulation, where it may play a direct role in regulating NFκB targets, or, most likely, 3) the small amount of nuclear TRAF2 interacts with the nuclear CD30v to drive NFκB activation. There is indeed evidence that TRAF2 (Min et al., 1998), TRAF6 (Pham et al., 2008), and IKKs, all initially believed to be obligatory cytoplasmic regulators of NFκB signaling, can enter the nucleus and interact with specific promoter regions, altering transcriptional activity and Histone-H3 phosphorylation (Yamamoto et al., 2003; Verma et al., 2004). Furthermore, the cytoplasmic form of CD40, the closest TNFR relative to CD30 was, like CD30v, also found in the nucleus and shown to possess transcriptional activity (Lin-Lee et al., 2006). We can only speculate as to what the role of nuclear CD30v may be, but it is not unlikely that it may play a role in a negative-feedback regulatory mechanism that self-limits CD30FL expression. CD30FL expression is indeed down-regulated upon expression of CD30v, and we show that this occurs independently of Thr-61. In cell types other than hESCs, CD30 promoter activity was shown to be controlled by AP-1, and we find that Thr-61 mutation does not affect CD30-mediated AP1 reporter activity or ERK activation. Wright and Duckett (2009) demonstrated that CD30FL expression can be regulated at a posttranslational level in the cytoplasm through interaction with ARNT and the CD30 C-terminus, leading to its accumulation in cytoplasmic vesicles. Our present data showing that CD30v is predominantly nuclear, does not interact with ARNT, and yet still leads to repression of CD30FL suggest this may be an alternative mechanism for CD30FL regulation independently of ARNT.

It is possible that nuclear CD30v interacts with a completely novel family of signaling molecules driving new phenotypes. Indeed, Ingenuity IPA analysis of our LC-MS data on proteins interacting with wild-type CD30v revealed that whereas most of these CD30-interacting proteins were nuclear proteins involved in cell cycle, cell death, and survival, as expected, we also identified proteins concentrated in nuclear speckles and paraspeckles with roles in RNA posttranscriptional modifications, such as ARL6IP4, HNRNPU, NUDT21, RBM39, and SRSF2 (Supplemental Table S4). Of note, ARL6IP4 is exclusively expressed during G_1/S transition and implicated in pre-mRNA splicing inhibition (Li et al., 2002); HNRNPU is known to promote MYC mRNA stabilization (Weidensdorfer et al., 2009); NUDT21 plays a key role in pre-mRNA 3′ cleavage and polyadenylation (Ruegsegger et al., 1996); RBM39 is a known transcriptional coactivator for steroid nuclear receptors ESR1/ER-α, ESR2/ER-β, and JUN/AP-1 and may be involved in pre-mRNA splicing process (Jung et al., 2002); and SRSF2 is necessary for the splicing of pre-mRNA and regulates cell cycle and apoptosis (Jang et al., 2009). In view of our data showing that CD30v-overexpressing cells possess substantially increased AP1 activity, C-MYC expression, increased rate of G_1/S transition, and reduced apoptosis, a novel role for CD30v involvement in RNA posttranscriptional modification seems plausible.

A prominent feature of hESCs that overexpress WT CD30v is the marked increase in cell proliferation rates. Indeed, WT CD30v-overexpressing hESCs display a higher proportion of cells in S phase, a concomitant decrease of cells in G_0/G_1, and a decreased G_2/M phase accompanied by reduced Histone-H3 phosphorylation. In agreement with this deregulation of the cell cycle in WT-CD30v–overexpressing hESCs, the cells express increased levels of C-MYC, C-FOS, and LIN28A, genes known to regulate cell cycle and proliferation and aid transformation (Singh and Dalton, 2009; Viswanathan et al., 2009; Li et al., 2012; Shyh-Chang and Daley, 2013), and CYCLIN A2, CYCLIN E1, and CDC25A, genes known to regulate G_1/S and G_2/M transitions (Murphy, 1999; Sandhu et al., 2000; Li et al., 2012). Of importance, mutation of Thr-61 causes reversion of both the altered cell cycle profile and the expression of these genes to a pattern identical to that of untransduced or control vector–transduced hESCs, indicating that the CD30v-mediated cell cycle changes are due to CD30-TRAF2–mediated NFκB signaling. What remain to be determined are the phosphorylation levels of the cyclins, which are known to be equally important for cell cycle control in hESCs (Singh and Dalton, 2009; Koledova, 2012).

We previously reported that CD30 expression inhibits H_2O_2-induced apoptosis of hESCs (Herszfeld et al., 2006). Here we show that overexpression of CD30v also protects hESCs from H_2O_2-induced apoptosis, as shown by the reduced levels of activated CASPASE-3 and cell death rates, and that mutation of Thr-61 in CD30v abolishes this protective effect, indicating that TRAF2-mediated canonical NFκB signaling downstream of CD30v is responsible for conferring the resistance to H_2O_2-induced apoptosis to hESC. We observed no differences in expression, intracellular localization, or transcription of TRAF2 between vector control, T61A, or WT CD30v-overexpressing hESCs, excluding the possibility that this effect is due to a CD30-mediated degradation of TRAF2 as reported in HEK-293 cells (Duckett and Thompson, 1997).

An increased rate of progression through the G_0/G_1 and G_2/M phases accompanied by a corresponding lengthening of the S phase and an ability to overcome H_2O_2-induced G_2 cell cycle arrest are characteristics indicative of transformation. CD30 has a pleiotropic effect on cell cycle and proliferation (Gruss et al., 1994; Pinto et al., 1996) and was shown to increase proliferation, modulate expression of cell cycle genes that accelerate G_1/S transition, and mediate evasion of growth inhibition in peripheral blood T-cells (Kadin et al., 2001), autoreactive γδT-cells (Levi et al., 2000), cutaneous CD30^{+} ALCL cell lines (Levi et al., 2000), and HL cells (Wendtner et al., 1995; Watanabe et al., 2011) via NFκB and ERK activation (Levi et al., 2000; Watanabe et al., 2011). Nonaka et al. (2005) implicated CD30 in cell transformation by showing that overexpression of CD30 in rat fibroblast at levels comparable with those in HL cells results in NFκB-dependent cell transformation. Our data show that TRAF2-mediated canonical NFκB signaling requiring Thr-61 in CD30v (and presumably Thr-524 in full length CD30) accelerates hESC proliferation and confers selective growth and survival advantages (Draper et al., 2004; Singh and Dalton, 2009). CD30-mediated enhancement of survival of cells that have accumulated genetic or epigenetic changes that would otherwise be committed to apoptosis may enhance the propensity of the stem cell population to accumulate further DNA mutations, develop genetic instability, and thus aid in the transformation of hESCs (Herszfeld et al., 2006; Harrison et al., 2009; Mateizel et al., 2009; Chung et al., 2010a,b, 2011). In this scenario, our data identifying the profound effects of mutating T61 on the CD30-NFκB signaling axis may allow for more efficient and specific ways to modulate this important signaling cascade to prevent such CD30-mediated adverse effects in hESCs,

using small molecules that target T61 in CD30, and as a corollary may provide novel therapeutic modalities for HL and ALCL.

MATERIALS AND METHODS

Cell culture

HES2, HES3, and HES4 cells were grown feeder-free in either KOSR (Life Technologies, Carlsbad, CA) or NutriStem (Stemgent, Cambridge, MA) with an additional 50 ng/ml basic fibroblast growth factor (b-FGF). Of note, ascorbate present in these media induces endogenous CD30FL and CD30v expression, as previously reported by our lab. We showed that ascorbic acid is the sole component in KOSR medium that induces CD30 expression (Chung et al., 2010a,b; Thakar and Wolvetang, 2014). Matrigel (Life Technologies) was diluted in ice-cold KO-DMEM/F12 at 0.0347 mg/cm^2 to coat tissue culture vessels before feeder-free culture. HES2 and HES4 hESCs that stably overexpress CD30v (CD30v^{OE}) were cultured alongside and compared with control HES2 and HES4 hESCs that do not express any endogenous CD30v and CD30FL (CD30$^-$). These CD30$^-$ and CD30v^{OE} hESCs were generated in the E.J.W.'s lab and grown feeder-free in mouse embryonic fibroblast (MEF)–conditioned KOSR minus ascorbate (Life Technologies) with 100 ng/ml b-FGF to ensure the absence of endogenous CD30FL and CD30V expression. For preparation of MEF conditioned medium (CM), irradiated (30-Gy γ-irradiation) MEF cells were seeded at 6×10^4 cells/cm^2 in MEF medium. After at least 4 h, the medium was replaced with either KOSR or KOSR minus ascorbate (0.3 ml/cm^2) supplemented with 4 ng/ml b-FGF. CM was collected daily for 7–10 d, filtered through a 0.22-μm filter, and supplemented with an additional 100 ng/ml b-FGF.

Cell cycle analysis

Cells were grown under pluripotency conditions as described earlier until they reached ~60% confluence, and medium was changed on cells 8 h before commencement of assay to ensure minimal external factors affecting cell cycle. BD Cycletest Plus DNA Reagent Kit (BD Biosciences, San Jose, CA) was used as per manufacturer's instructions to assess cell cycle. Analysis of the percentage of cells under each cell cycle phase was carried out using FCS4 Express software. Phospho-Histone H3 (Ser-10; 1:50; Cell Signaling Technology, Boston, MA) expression was measured using flow cytometry to determine the percentage of cells undergoing mitosis. Cell counts were also performed for assessing proliferation. Equal numbers of cells were seeded into each of the six wells of a 24-well plate per condition (WT, T61A, and OE V/C). Each subsequent day, cells were dissociated from one well in each condition using TrypleE (Life Technologies) and counted subsequently using TC10 Automated Cell Counter (Bio-Rad Laboratories, Hercules, CA) as per manufacturer's instructions.

Plasmids and generation of mutant and WT cells

We cloned the WT-CD30vOE (Wild-Type CD30-Variant Over-Expression) cDNA sequence into pENTR 5′-TOPO TA vector using a pENTR 5′-TOPO TA cloning kit (Life Technologies). We then generated specific mutations (putative SUMOylation and USP7-binding sites) and deletions (putative SH2- and FHA-binding sites) using the Change-IT Multiple Mutation Site Directed Mutagenesis Kit (USB, Cleveland, OH). To facilitate generation of WT and mutant CD30v mammalian expression constructs, AGE1 (5′) and SAL1 (3′) restriction sites were added to the Addgene plasmid 12252: pRRLSIN.cPPT.PGK-GFP.WPRE (Didier Trono, Head of Laboratory of Virology and Genetics, EPFL School of Life Sciences).

We next generated N-terminally HA-tagged WT and mutant CD30vOE (T61_A, T66_A, and T61_66A) mammalian-expression

plasmids. Mutagenic primers and complementary primers were designed to mutate the threonine residues at positions 61 and 66 individually and simultaneously using the Change-IT Multiple Mutation Site Directed Mutagenesis Kit (USB). All primer sequences used are described in Supplemental Table S1.

293FT cells were transfected with the lentiviral vector DNA, pCMV Δ8.2, and pLP$VSVG$ plasmids using Lipofectamine 2000 (all from Life Technologies), and virus was collected 36 h posttransfection. This virus was then used to transduce desired cells for 24 h in presence of 7 μg/ml Polybrene (Sigma-Aldrich, St. Louis, MO). Cells were cultured normally for 5 d, after which they were selected using 2 μg/ml puromycin (Sigma-Aldrich). Resistant colonies were picked after 4 d and expanded. siTRAF2 (Sigma-Aldrich) was used at a final 50 nM concentration.

HA-tag immunoprecipitation and mass spectrophotometry

HA-tagged WT-CD30vOE and mutant T61_A CD30vOE cells, along with untagged-EGFP–expressing cells, were quickly washed with cold PBS+ (Life Technologies) twice, and 200 μl of 1× Cell Lysis Buffer (Cell Signaling Technology) containing 1 mM phenylmethylsulfonyl fluoride (Sigma-Aldrich) and 1× phosphatase and protease inhibitors (F. Hoffmann-La Roche AG, Basel, Switzerland) were added per well of a six-well plate to at least four wells. Two duplicate wells were used for RNA and protein collection. The plate was incubated on ice for 5 min, cells were scraped, and the resulting lysate was passed through a 30-gauge syringe multiple times and centrifuged at $14,000 \times g$ for 15 min twice at 4°C, and the supernatant was collected. A 100-μl amount was used for Western blot analysis, and 600 μl was used for immunoprecipitation using the Pierce HA Tag IP/Co-IP Kit (Thermo Fisher Scientific, Waltham, MA), following the manufacturer's instructions. A 30-μl amount of eluate pooled was immediately neutralized with 1.5 μl of 1 M Tris, pH 9.5, and mass-spectrophotometric analysis was subsequently carried out.

Sample processing for tandem mass spectrometry

A 20-μl amount of the affinity eluate was reduced by the addition of NH$_4$HCO$_3$ (Sigma-Aldrich) to 50 mM SDS (Bio-Rad) to 2% and dithiothreitol (GE Healthcare, Little Chalfont, UK) to 20 mM. Samples were incubated for 16 h at 4°C, followed by 2 h at 22°C. The reduced proteins were then alkylated by the addition of iodoacetamide (GE Healthcare) to 50 mM and incubated at 22°C in the dark for 2 h. Protein was precipitated by acid precipitation (2-D Clean-up Kit; GE Healthcare) with an overnight final wash step to ensure the removal of all acid. Precipitated proteins were resuspended in 30 μl of 10% acetonitrile (J.T. Baker, Center Valley, PA) and 40 mM NH$_4$HCO$_3$ and digested with 0.5 μg of modified sequencing-grade trypsin and bovine pancreas (Roche) for 2 h at 37°C, followed by the addition of a further 0.5 μg of trypsin and incubation for 6 h at 37°C. The digest liquor was removed in vacuo and the residue reconstituted in 30 μl of 1% formic acid and 2% acetonitrile.

Tandem mass spectrometry. Acidified digests were analyzed by nano–high-performance liquid chromatography–tandem mass spectrometry using a Prominence nano HPLC system (Shiumadsu, Kyoto, Japan) interfaced with an Orbitrap Elite hybrid mass spectrometer (Thermo Fischer Scientific, Bremen, Germany). Digests were loaded onto a Reprosil aq C18 3-μm, 120-A, 300-μm trap (SGE pn-2222066) at 30 μl/min in 2% acetonitrile (ACN) and 0.1% (vol/vol) aqueous formic acid for 3.5 min at 50°C, then switched in-line with an analytical column (15 cm × 75 μm fused silica, self-packed) Reprosil aq C18 2.4-um (pn-r124.aq batch-9756, Dr. Maisch GmbH, Ammerbuch-Entringen, Germany) using a flow rate of 0.3 μl/min

and 98% solvent A (0.1% [vol/vol] aqueous formic acid), 2% solvent B (80% [vol/vol] ACN, 0.1% [vol/vol] aqueous formic acid). Peptides were separated at 50°C using a sequence of linear gradients: to 15% B over 5 min; to 47% B over 90 min; to 95% B over 10 min; and then holding the column at 95% B for 5 min. Eluate from the analytical column was introduced into the Orbitrap Elite throughout the entire run via a Nanospray Flex Ion Source (Thermo Fisher Scientific) and a 10-μm-inner-diameter uncoated silica emitter (New Objective, Woburn, MA). Typical spray voltage was 1.4 kV with no sheath, sweep, or auxiliary gases used. The heated capillary temperature was set to 285°C. The Orbitrap Elite was controlled using Xcalibur 2.2 software (Thermo Fisher Scientific) and operated in a data-dependent acquisition mode to automatically switch between Orbitrap-MS and ion trap-MS/MS. The survey full-scan mass spectra (from m/z 380 to 1700) were acquired in the Orbitrap with resolving power set to 240,000 (at 400 m/z) after accumulating ions to an automatic gain control (AGC) target value of 1.0×10^6 charges in the LTQ. MS/MS spectra were concurrently acquired on the 15 most intense ions from the survey scan in the LTQ filled to an AGC target value of 3.0×10^4. Charge-state filtering, by which unassigned and charge state 1 precursor ions were not selected for fragmentation, and dynamic exclusion (repeat count 1, repeat duration 30 s, exclusion list size 500, exclusion duration 90 s) were used. Fragmentation conditions in the LTQ were 35% normalized collision energy; activation q of 0.25; 10-ms activation time; and minimum ion selection intensity, 5000 counts. Maximum ion injection times were 200 ms for survey full scans and 50 ms for MS/MS.

Data processing. Tandem mass spectra were processed using Proteome Discoverer (version 1.3; Thermo Fisher Scientific) and submitted to Mascot (version 2.2.06; Matrix Science, London, UK) with the following parameters specified: fixed modification, carbamidomethyl-cysteine; variable modifications, deamidation (asparagine, glutamine) and oxidation (methionine); enzyme, trypsin; two missed cleavages; database, Uniprot human reference proteome (20120228) and bovine trypsin (65837 entries); MS tolerance, 10 ppm; MSMS tolerance, 0.8 Da.

Scaffold (version 3.6.4, Proteome Software, Portland, OR; Searle, 2010) was used to validate Mascot protein identifications and compare across samples. Scaffold probabilistically validates these peptide identifications using PeptideProphet (Keller *et al.*, 2002) and derives corresponding protein probabilities using ProteinProphet (Nesvizhskii *et al.*, 2003). Two peptides per protein with ≥95% probability and an overall protein probability of ≥99% were required to assign a protein or protein group.

Western blot analysis
Cells were washed with phosphate-buffered saline (PBS) twice and subsequently lysed with 5× loading buffer (130 mM Tris, pH 6.8, 4% SDS, 0.02% bromophenol blue, 20% glycerol, 100 mM dithiothreitol) containing 10% PhosSTOP phosphatase inhibitor (Roche), homogenized with 30-guage syringe needles, heated at 80°C for 10 min, and resolved using SDS–PAGE. The iBlot Dry Blotting System (Life Technologies) was used to transfer proteins onto a polyvinylidene fluoride membrane. Blots were blocked in blocking buffer (Tris-buffered saline, 0.01% Tween-20, 5% bovine serum albumin [BSA]) at room temperature for 2 h, probed with desired primary antibodies in blocking buffer at 4°C overnight with gentle agitation, washed three times for 15 min each, probed with appropriate secondary antibodies in blocking buffer for 1 h at room temperature, washed as before, and detected using the Pierce ECL Western Blotting detection kit according to manufacturer's recommenda-

tions (Thermo Fisher Scientific) on either Typhoon (GE Healthcare) or V3-Western Workflow (Bio-Rad) for a densitometric representation. The images were respectively analyzed using either One-Rad (Bio-Rad) or Image Lab (Bio-Rad) software. All antibodies with working dilutions are described in Supplemental Table S2. Cytoplasmic and nuclear fractionation of cell lysates was carried out using NE-PER Nuclear and Cytoplasmic Extraction Reagents (Thermo Fisher Scientific) according to the manufacturer's instructions.

Immunofluorescence assays
Cells were washed three times with PBS, fixed with 3% paraformaldehyde, permeabilized with chilled 100% methanol at –20°C for 10 min, blocked in blocking buffer (5% BSA, 5% goat serum, 0.2% sodium azide, 0.3% Triton X-100 in PBS) for 1 h at room temperature, and incubated with desired primary antibodies overnight at 4°C. Next cells were washed three times with PBS and incubated for 2 h at room temperature in the dark with species- and isotype-matched Alexa Fluor–conjugated secondary antibodies (1:1000; Life Technologies), washed as before, mounted with ProLong Gold antifade reagent with 4′,6-diamidino-2-phenylindole (DAPI; Life Technologies), coverslipped, and sealed using nail polish. The cells were cured for 24 h at room temperature and then examined for staining using either using a QImaging-Retiga-EXi Fast 1394 fluorescence microscope or Carl Zeiss LSM 710 for confocal microscopy at room temperature. Images were acquired with equal exposure and gain settings and were equally adjusted for brightness or contrast postacquisition. Secondary antibody–only treated cells were used as negative control. All antibodies with working dilutions are described in Supplemental Table S2.

H₂O₂ sensitivity assays
Cells were grown under pluripotency conditions as described earlier until they reached ~70% confluence in a six-well plate (for cell cycle and PI-based survival assays) or eight-well chamber slide (for immunofluorescence assay), and medium was changed 8 h before commencement of the assay. Cells were then subjected to 200 μM H_2O_2 for 3 h for immunofluorescence assay to detect active CASPASE-3 expression. Cells were also subjected to 100 μM H_2O_2 for 24 h to assess cell death via PI-based fluorescence assay and cell cycle. After H_2O_2 treatment, medium was pooled, and then the remaining cells were washed in PBS and dissociated and added to the pooled medium, spun, and resuspended in PBS. Half of the cells were subsequently stained with PI to measure cell death, and the other half was used to assess cell cycle using BD Cycletest Plus DNA Reagent Kit (BD Biosciences) as per manufacturer's instructions. All antibodies with working dilutions are described in Supplemental Table S2.

Luciferase assays
HES3 cells were cultured in a 96-well plate and transfected with a mixture of 33 ng of β-galactosidase and either 33 ng of NFκB-luciferase or 33 ng of AP1-luciferase expression plasmids with 0.15 μl of Fugene-6 (Roche) to analyze NFκB or AP1 reporter activity 48 h posttransfection. To that mix either 33 ng of CD30 plasmid (wild-type and various mutants) or 33 ng of siRNAs (TRAF2 or GFP) was added. These cells were next washed once with PBS and lysed with 150 μl of 1× Passive Lysis Buffer (Promega, Madison, WI). For luciferase assay, 50 μl of cell lysate was transferred to a white 96-well plate, and 100 μl of freshly dissolved luciferase assay buffer (E1501; Promega) was added per well and luminescence was read immediately on a SpectraMax M5 Microplate Reader (Molecular Devices, Sunnyvale, CA) to measure either NFκB or AP1 activity. For

β-galactosidase activity assessment (for normalization of well-to-well differences in transfection efficiency), 50 μl of cell lysate was transferred to a clear 96-well plate, and 100 μl of 1.5× β-galactosidase assay buffer was added per well. The plate was incubated at 37°C for 2 h and detected subsequently on SpectraMax M5 Microplate Reader. Each condition was performed in quintuplicate on each plate.

RNA isolation, cDNA synthesis, and quantitative PCR analysis

Total RNA was prepared using the RNA Purification kit (Macherey-Nagel, Bethlehem, PA), and 1 μg of RNA was converted to cDNA in a 10-μl reaction mix with iScript cDNA synthesis kit (Bio-Rad), both according to manufacturer's protocol. Quantitative PCRs used SsoFast EvaGreen Supermix (Bio-Rad) with cDNA template (from ~5 ng of RNA equivalent/reaction) according to manufacturer's instructions using a C1000 Thermal Cycler (Bio-Rad). All primer sequences are listed in Supplemental Table S1. The expression value of each gene was normalized to a human β-actin control (Life Technologies). Relative gene expression was analyzed using software C-1000 (Bio-Rad) and the ΔΔCt method as described in Livak and Schmittgen (2001) and Briggs et al. (2012).

Flow cytometry analysis

Flow cytometry was performed on hESCs cultures in KOSR as previously described (Briggs et al., 2012), using appropriate primary antibodies as described in Supplemental Table S2. Species- and isotype-matched Alexa Fluor–conjugated secondary antibodies (1:1000; Life Technologies) were used. Appropriate isotype control antibodies diluted at an identical final concentration as the primary antibodies were used as negative control for the experiments. Stained cells were analyzed by flow-cytometry using Accuri C6 FACS analyzer (BD Biosciences).

SUMOylation assay

SUMOylation assay was carried out using a SUMOlink in vitro SUMOylation assay kit (Active Motif, Carlsbad, CA). The assay was set up according to the manufacturer's instructions. A 4.5-μg amount of CD30v protein was used for SDS–PAGE analysis, blocked, and subsequently stained with primary and secondary antibodies according to manufacturer's instructions. Detection was carried out using Pierce ECL Western Blotting detection according to the manufacturer's recommendation (Thermo Fisher Scientific) on a Typhoon Scanner (GE Healthcare).

Protein sequence and structure analysis

The sequence of CD30 was analyzed by Web-hosted bioinformatics tools for similarities to other proteins: Blast (Altschul et al., 1990); T-Coffee (Notredame et al., 2000); secondary structure prediction (Jpred; Cuff and Barton, 2000); prediction of disordered regions (GeneSilico MetaDisorder; Kozlowski and Bujnicki, 2012); and fold recognition (I-Tasser; Roy et al., 2010). The structure prediction method I-Tasser (Roy et al., 2010) predicts that CD30v could fold into a compact α/β domain, but the confidence of the prediction is very low. A homology model of TRAF2:CD30 fragment was prepared using Modeller 9.9 (Eswar et al., 2008) based on the structures of TRAF3:CD40 fragment (Protein Data Bank [PDB] ID: 1FLL; Ni et al., 2000) and TRAF2:CD30 fragment (PDB ID: 1D01; Ye et al., 1999). For the preparation of the homology model, the sequences of CD30 and CD40 were aligned based on the structural superposition of TRAF2 and TRAF3 in the two structures.

Statistical analysis

Data represent mean ± SD of the number (n) of independent experiments unless indicated otherwise. Statistical significance was calculated by a two-way analysis of variance (ANOVA) with Bonferroni posttests to compare replicate means between the indicated groups for all experiments, with the exception of phospho–Histone H3 quantification, for which one-way ANOVA with Dunnett posttest was used.

REFERENCES
Aizawa S, Nakano H, Ishida T, Horie R, Nagai M, Ito K, Yagita H, Okumura K, Inoue J, Watanabe T (1997). Tumor necrosis factor receptor-associated factor (TRAF) 5 and TRAF2 are involved in CD30-mediated NFkappaB activation. J Biol Chem 272, 2042–2045.

Altschul SF, Gish W, Miller W, Myers EW, Lipman DJ (1990). Basic local alignment search tool. J Mol Biol 215, 403–410.

Amin HM, Lai R (2007). Pathobiology of ALK(+) anaplastic large-cell lymphoma. Blood 110, 2259–2267.

Armstrong L, Hughes O, Young S, Hyslop L, Stewart R, Wappler I, Peters H, Walter T, Stojkovic P, Evans J, et al. (2006). The role of PI3K/AKT, MAPK/ERK and NFκβ signalling in the maintenance of human embryonic stem cell pluripotency and viability highlighted by transcriptional profiling and functional analysis. Hum Mol Genet 15, 1894–1913.

Briggs JA, Sun J, Shepherd J, Ovchinnikov DA, Chung TL, Nayler SP, Kao LP, Morrow CA, Thakar NY, Soo SY, et al. (2012). Integration-free induced pluripotent stem cells model genetic and neural developmental features of Down syndrome etiology. Stem Cells 31, 467–478.

Buchan SL, Al-Shamkhani A (2012). Distinct motifs in the intracellular domain of human CD30 differentially activate canonical and alternative transcription factor NF-κB signaling. PLoS One 7, e45244.

Chung T-L, Brena RM, Kolle G, Grimmond SM, Berman BP, Laird PW, Pera MF, Wolvetang EJ (2010a). Vitamin C promotes widespread yet specific DNA demethylation of the epigenome in human embryonic stem cells. Stem Cells 28, 1848–1855.

Chung T-L, Thaker NY, Wolvetang EJ (2011). Genetic and epigenetic instability of human pluripotent stem cells. Open Stem Cell J 3, 52–61.

Chung T-L, Turner JP, Thaker NY, Kolle G, Cooper-White JJ, Grimmond SM, Pera MF, Wolvetang EJ (2010b). Ascorbate promotes epigenetic activation of CD30 in human embryonic stem cells. Stem Cells 28, 1782–1793.

Cuff JA, Barton GJ (2000). Application of multiple sequence alignment profiles to improve protein secondary structure prediction. Proteins 40, 502–511.

Draper JS, Smith K, Gokhale P, Moore HD, Maltby E, Johnson J, Meisner L, Zwaka TP, Thomson JA, Andrews PW (2004). Recurrent gain of chromosomes 17q and 12 in cultured human embryonic stem cells. Nat Biotechnol 22, 53–54.

Duckett CS, Thompson CB (1997). CD30-dependent degradation of TRAF2: implications for negative regulation of TRAF signaling and the control of cell survival. Genes Dev 11, 2810–2821.

Durkop H, Foss HD, Eitelbach F, Anagnostopoulos I, Latza U, Pileri S, Stein H (2000). Expression of the CD30 antigen in non-lymphoid tissues and cells. J Pathol 190, 613–618.

Durkop H, Latza U, Hummel M, Eitelbach F, Seed B, Stein H (1992). Molecular cloning and expression of a new member of the nerve growth factor receptor family that is characteristic for Hodgkin's disease. Cell 68, 421–427.

Eswar N, Eramian D, Webb B, Shen MY, Sali A (2008). Protein structure modeling with MODELLER. Methods Mol Biol 426, 145–159.

Gedrich RW, Gilfillan MC, Duckett CS, Van Dongen JL, Thompson CB (1996). CD30 contains two binding sites with different specificities for members of the tumor necrosis factor receptor-associated factor family of signal transducing proteins. J Biol Chem 271, 12852–12858.

Gruss H, Boiani N, Williams D, Armitage R, Smith C, Goodwin R (1994). Pleiotropic effects of the CD30 ligand on CD30-expressing cells and lymphoma cell lines. Blood 83, 2045–2056.

Harrison NJ, Barnes J, Jones M, Baker D, Gokhale PJ, Andrews PW (2009). CD30 expression reveals that culture adaptation of human embryonic stem cells can occur through differing routes. Stem Cells 27, 1057–1065.

Hat B, Puszynski K, Lipniacki T (2009). Exploring mechanisms of oscillations in p53 and nuclear factor-kappa B systems. IET Syst Biol 3, 342–355.

Herszfeld D, Wolvetang E, Langton-Bunker E, Chung T-L, Filipczyk AA, Houssami S, Jamshidi P, Koh K, Laslett AL, Michalska A, et al. (2006). CD30 is a survival factor and a biomarker for transformed human pluripotent stem cells. Nat Biotechnol 24, 351–357.

Hirsch B, Hummel M, Bentink S, Fouladi F, Spang R, Zollinger R, Stein H, Durkop H (2008). CD30-induced signaling is absent in hodgkin's cells but present in anaplastic large cell lymphoma cells. Am J Pathol 172, 510–520.

Horie R, Aizawa S, Nagai M, Ito K, Higashihara M, Ishida T, Inoue J, Watanabe T (1998). A novel domain in the CD30 cytoplasmic tail mediates NFkappaB activation. Int Immunol 10, 203–210.

Horie R, Gattei V, Ito K, Imajo-Ohmi S, Tange T, Miyauchi J, Pinto A, Degan M, De Iuliis A, Tassan Mazzocco F, et al. (1999). Frequent expression of the variant CD30 in human malignant myeloid and lymphoid neoplasms. Am J Pathol 155, 2029–2041.

Horie R, Ito K, Tatewaki M, Nagai M, Aizawa S, Higashihara M, Ishida T, Inoue J, Takizawa H, Watanabe T (1996). A variant CD30 protein lacking extracellular and transmembrane domains is induced in HL-60 by tetradecanoylphorbol acetate and is expressed in alveolar macrophages. Blood 88, 2422–2432.

Horie R, Watanabe T (1998). CD30: expression and function in health and disease. Semin Immunol 10, 457–470.

Horie R, Watanabe T, Morishita Y, Ito K, Ishida T, Kanegae Y, Saito I, Higashihara M, Mori S, Kadin ME (2002). Ligand-independent signaling by overexpressed CD30 drives NF-kappaB activation in Hodgkin-Reed-Sternberg cells. Oncogene 21, 2493–2503.

Jang SW, Liu X, Fu H, Rees H, Yepes M, Levey A, Ye K (2009). Interaction of Akt-phosphorylated SRPK2 with 14–3-3 mediates cell cycle and cell death in neurons. J Biol Chem 284, 24512–24525.

Jung DJ, Na SY, Na DS, Lee JW (2002). Molecular cloning and characterization of CAPER, a novel coactivator of activating protein-1 and estrogen receptors. J Biol Chem 277, 1229–1234.

Kadin ME, Levi EDI, Kempf W (2001). Progression of lymphomatoid papulosis to systemic lymphoma is associated with escape from growth inhibition by transforming growth factor-β and CD30 ligand. Ann NY Acad Sci 941, 59–68.

Keller A, Nesvizhskii AI, Kolker E, Aebersold R (2002). Empirical statistical model to estimate the accuracy of peptide identifications made by MS/MS and database search. Anal Chem 74, 5383–5392.

Koledova Z (2012). Self-renewal of embryonic stem cells: cell cycle regulation. In: Stem Cells and Cancer Stem Cells, Vol. 6, ed. MA Hayat, Dordrecht, Netherlands: Springer, 11–20.

Kozlowski LP, Bujnicki JM (2012). MetaDisorder: a meta-server for the prediction of intrinsic disorder in proteins. BMC Bioinformatics 13, 111.

Levi E, Wang Z, Petrogiannis-Haliotis T, Pfeifer WM, Kempf W, Drews R, Kadin ME (2000). Distinct effects of CD30 and Fas signaling in cutaneous anaplastic lymphomas: a possible mechanism for disease progression. J Invest Dermatol 115, 1034–1040.

Li N, Zhong X, Lin X, Guo J, Zou L, Tanyi JL, Shao Z, Liang S, Wang L-P, Hwang W-T, et al. (2012). Lin-28 homologue A (LIN28A) promotes cell cycle progression via regulation of cyclin-dependent kinase 2 (CDK2), cyclin D1 (CCND1), and cell division cycle 25 homolog A (CDC25A) expression in cancer. J Biol Chem 287, 17386–17397.

Li Q, Zhao H, Jiang L, Che Y, Dong C, Wang L, Wang J, Liu L (2002). An SR-protein induced by HSVI binding to cells functioning as a splicing inhibitor of viral pre-mRNA. J Mol Biol 316, 887–894.

Lin-Lee YC, Pham LV, Tamayo AT, Fu L, Zhou HJ, Yoshimura LC, Decker GL, Ford RJ (2006). Nuclear localization in the biology of the CD40 receptor in normal and neoplastic human B lymphocytes. J Biol Chem 281, 18878–18887.

Livak KJ, Schmittgen TD (2001). Analysis of relative gene expression data using real-time quantitative PCR and the 2−ΔΔCT method. Methods 25, 402–408.

Mateizel I, Spits C, Verloes A, Mertzanidou A, Liebaers I, Sermon K (2009). Characterization of CD30 expression in human embryonic stem cell lines cultured in serum-free media and passaged mechanically. Hum Reprod 24, 2477–2489.

Min W, Bradley JR, Galbraith JJ, Jones SJ, Ledgerwood EC, Pober JS (1998). The N-terminal domains target TNF receptor-associated factor-2 to the nucleus and display transcriptional regulatory activity. J Immunol 161, 319–324.

Murphy M (1999). Delayed early embryonic lethality following disruption of the murine cyclin A2 gene. Nat Genet 23, 481.

Nesvizhskii AI, Keller A, Kolker E, Aebersold R (2003). A statistical model for identifying proteins by tandem mass spectrometry. Anal Chem 75, 4646–4658.

Ni CZ, Welsh K, Leo E, Chiou CK, Wu H, Reed JC, Ely KR (2000). Molecular basis for CD40 signaling mediated by TRAF3. Proc Natl Acad Sci USA 97, 10395–10399.

Nonaka M, Horie R, Itoh K, Watanabe T, Yamamoto N, Yamaoka S (2005). Aberrant NF-[kappa]B2//p52 expression in Hodgkin//Reed-Sternberg cells and CD30-transformed rat fibroblasts. Oncogene 24, 3976–3986.

Notredame C, Higgins DG, Heringa J (2000). T-Coffee: A novel method for fast and accurate multiple sequence alignment. J Mol Biol 302, 205–217.

Pera MF, Bennett W, Cerretti DP (1997). Expression of CD30 and CD30 ligand in cultured cell lines from human germ-cell tumors. Lab Invest 76, 497–504.

Pham LV, Zhou H-J, Lin-Lee Y-C, Tamayo AT, Yoshimura LC, Fu L, Darnay BG, Ford RJ (2008). Nuclear tumor necrosis factor receptor-associated factor 6 in lymphoid cells negatively regulates c-Myb-mediated transactivation through small ubiquitin-related modifier-1 modification. J Biol Chem 283, 5081–5089.

Pinto A, Aldinucci D, Gloghini A, Zagonel V, Degan M, Improta S, Juzbasic S, Todesco M, Perin V, Gattei V, et al. (1996). Human eosinophils express functional CD30 ligand and stimulate proliferation of a Hodgkin's disease cell line. Blood 88, 3299–3305.

Roy A, Kucukural A, Zhang Y (2010). I-TASSER: a unified platform for automated protein structure and function prediction. Nat Protoc 5, 725–738.

Ruegsegger U, Beyer K, Keller W (1996). Purification and characterization of human cleavage factor Im involved in the 3′ end processing of messenger RNA precursors. J Biol Chem 271, 6107–6113.

Sandhu C, Donovan J, Bhattacharya N, Stampfer M, Worland P, Slingerland J (2000). Reduction of Cdc25A contributes to cyclin E1-Cdk2 inhibition at senescence in human mammary epithelial cells. Oncogene 19, 5314–5323.

Schneider C, Hübinger G (2002). Pleiotropic signal transduction mediated by human CD30: a member of the tumor necrosis factor receptor (TNFR) family. Leuk Lymphoma 43, 1355–1366.

Searle BC (2010). Scaffold: a bioinformatic tool for validating MS/MS-based proteomic studies. Proteomics 10, 1265–1269.

Shyh-Chang N, Daley, George Q (2013). Lin28: primal regulator of growth and metabolism in stem cells. Cell Stem Cell 12, 395–406.

Singh AM, Dalton S (2009). The cell cycle and Myc intersect with mechanisms that regulate pluripotency and reprogramming. Cell Stem Cell 5, 141–149.

Smith CA, Gruss HJ, Davis T, Anderson D, Farrah T, Baker E, Sutherland GR, Brannan CI, Copeland NG, Jenkins NA, et al. (1993). CD30 antigen, a marker for Hodgkin's lymphoma, is a receptor whose ligand defines an emerging family of cytokines with homology to TNF. Cell 73, 1349–1360.

Thakar NY, Wolvetang EJ (2014). Ascorbate as a modulator of the epigenome. In: Nutrition and Epigenetics, CRC Press, 199–218.

Verma UN, Yamamoto Y, Prajapati S, Gaynor RB (2004). Nuclear role of IκB kinase-γ/NF-κB essential modulator (IKKγ/NEMO) in NF-κB-dependent gene expression. J Biol Chem 279, 3509–3515.

Viswanathan SR, Powers JT, Einhorn W, Hoshida Y, Ng TL, Toffanin S, O'Sullivan M, Lu J, Phillips LA, Lockhart VL, et al. (2009). Lin28 promotes transformation and is associated with advanced human malignancies. Nat Genet 41, 843–848.

Watanabe M, Nakano K, Togano T, Nakashima M, Higashihara M, Kadin ME, Watanabe T, Horie R (2011). Targeted repression of overexpressed CD30 downregulates NF-kappaB and ERK1/2 pathway in Hodgkin lymphoma cell lines. Oncol Res 19, 463–469.

Watanabe M, Sasaki M, Itoh K, Higashihara M, Umezawa K, Kadin ME, Abraham LJ, Watanabe T, Horie R (2005). JunB induced by constitutive CD30-extracellular signal-regulated kinase 1/2 mitogen-activated protein kinase signaling activates the CD30 promoter in anaplastic large cell lymphoma and reed-sternberg cells of Hodgkin lymphoma. Cancer Res 65, 7628–7634.

Weidensdorfer D, Stohr N, Baude A, Lederer M, Kohn M, Schierhorn A, Buchmeier S, Wahle E, Huttelmaier S (2009). Control of c-myc mRNA stability by IGF2BP1-associated cytoplasmic RNPs. RNA 15, 104–115.

Wendtner C-M, Schmitt B, Gruss H-J, Druker BJ, Emmerich B, Goodwin RG, Hallek M (1995). CD30 ligand signal transduction involves activation of a tyrosine kinase and of mitogen-activated protein kinase in a Hodgkin's lymphoma cell line. Cancer Res 55, 4157–4161.

Wright CW, Duckett CS (2009). The aryl hydrocarbon nuclear translocator alters CD30-mediated NF-κB-dependent transcription. Science 323, 251–255.

Wright CW, Rumble JM, Duckett CS (2007). CD30 activates both the canonical and alternative NF-kappaB pathways in anaplastic large cell lymphoma cells. J Biol Chem 282, 10252–10262.

Yamamoto Y, Verma UN, Prajapati S, Kwak Y-T, Gaynor RB (2003). Histone H3 phosphorylation by IKK-α is critical for cytokine-induced gene expression. Nature 423, 655–659.

Yang C, Atkinson SP, Vilella F, Lloret M, Armstrong L, Mann DA, Lako M (2010). Opposing putative roles for canonical and noncanonical NFκB Signaling on the survival, proliferation, and differentiation potential of human embryonic stem cells. Stem Cells 28, 1970–1980.

Ye H, Park YC, Kreishman M, Kieff E, Wu H (1999). The structural basis for the recognition of diverse receptor sequences by TRAF2. Mol Cell 4, 321–330.

Zheng B, Fiumara P, Li YV, Georgakis G, Snell V, Younes M, Vauthey JN, Carbone A, Younes A (2003). MEK/ERK pathway is aberrantly active in Hodgkin disease: a signaling pathway shared by CD30, CD40, and RANK that regulates cell proliferation and survival. Blood 102, 1019–1027.